J|A|C|S ARTICLES

Published on Web 12/01/2010

Mechanism of Alcohol Oxidation by Dipicolinate Vanadium(V): Unexpected Role of Pyridine

Susan K. Hanson,* R. Tom Baker,‡ John C. Gordon, Brian L. Scott, L. A. "Pete" Silks, and David L. Thorn

Chemistry, Bioscience, and Materials Physics Applications Divisions, Los Alamos National Laboratory, Los Alamos, New Mexico 87544, United States

Received June 29, 2010; E-mail: skhanson@lanl.gov

Abstract: Dipicolinate vanadium(V) alkoxide complexes (dipic)V^{V}(O)(OR) (OR = isopropoxide (**1**), *n*-butanoxide (**2**), cyclobutanoxide (**3**), and α-*tert*-butylbenzylalkoxide (**4**)) react with pyridine to afford vanadium(IV) and 0.5 equiv of an aldehyde or ketone product. The role of pyridine in the reaction has been investigated. Both NMR and X-ray crystallography experiments indicate that pyridine coordinates to **1**, which is in equilibrium with (dipic)V^{V}(O)(O^{i}Pr)(pyr) (**1-Pyr**). Kinetic studies of the alcohol oxidation suggest a pathway where the rate-limiting step is bimolecular and involves attack of pyridine on the C−H bond of the isopropoxide ligand of **1** or **1-Pyr**. The oxidations of mechanistic probes cyclobutanol and α-*tert*-butylbenzylalcohol support a two-electron pathway proceeding through a vanadium(III) intermediate. The alcohol oxidation reaction is promoted by more basic pyridines and facilitated by electron-withdrawing substituents on the dipicolinate ligand. The involvement of base in the elementary alcohol oxidation step observed for the dipicolinate system is an unprecedented mechanism for vanadium-mediated alcohol oxidation and suggests new ways to tune reactivity and selectivity of vanadium catalysts.

Introduction

Catalytic aerobic oxidation of alcohols is an attractive method for the synthesis of ketones, aldehydes, and carboxylic acids. Using air as an oxidant offers significant environmental and economic benefits over traditional stoichiometric oxidants like potassium permanganate, chromium- and DMSO-based reagents, and Dess−Martin periodinane.[1−3] Since the initial discovery of palladium-catalyzed aerobic alcohol oxidation reported by Blackburn and Schwartz, more recent work by Uemura, Stahl, Sigman, Stoltz, and others has described highly effective palladium catalysts that operate under mild conditions.[4−10] Extensive investigations of the palladium systems have given rise to significant advances both in optimizing known catalysts and more importantly, the discovery of new catalysts.[6−8] In general, mechanistic studies of the palladium systems support a pathway involving coordination of alcohol to the palladium center and deprotonation of the coordinated alcohol by base, followed by β-hydride elimination to generate a palladium(II) hydride intermediate.[2,8]

Recently, a number of base metal catalysts for aerobic alcohol oxidation have been uncovered, including copper and vanadium complexes.[3,11−14] The use of earth-abundant metals is advantageous in terms of catalyst cost and availability, but these metals typically react by different mechanisms than their precious-metal counterparts. For example, a hydrogen atom abstraction pathway is often invoked for the reactions of copper complexes.[15−17] The mechanism of alcohol oxidation has important ramifications for the reaction selectivity; a copper dimer of redox-active phenolate ligands reported by Wieghardt and co-workers is thought to react by hydrogen atom abstraction and catalyzes the oxidation of secondary alcohols to ketones and diols.[18]

Vanadium complexes are also emerging as promising catalysts for aerobic alcohol oxidation. Uemura and co-workers reported the aerobic oxidation of phenyl- and alkyl-substituted

‡ Current address: Department of Chemistry and Centre for Catalysis Research and Innovation, University of Ottawa, Ottawa, ON, Canada K1N 6N5.

(1) Punniyamurthy, T.; Velusamy, S.; Iqbal, J. *Chem. Rev.* **2005**, *105*, 2329–2363.
(2) Stahl, S. S. *Angew. Chem., Int. Ed.* **2004**, *43*, 3400–3420.
(3) Schultz, M. J.; Sigman, M. S. *Tetrahedron* **2006**, *62*, 8227–8241.
(4) Blackburn, T. F.; Schwartz, J. *J. Chem. Soc., Chem. Commun.* **1977**, 157–158.
(5) Nishimura, T.; Onoue, T.; Ohe, K.; Uemura, S. *J. Org. Chem.* **1999**, *64*, 6750–6755.
(6) Steinhoff, B. A.; King, A. E.; Stahl, S. S. *J. Org. Chem.* **2006**, *71*, 1861–1868.
(7) Steinhoff, B. A.; Stahl, S. S. *J. Am. Chem. Soc.* **2006**, *128*, 4348–4355.
(8) Sigman, M. S.; Jensen, D. R. *Acc. Chem. Res.* **2006**, *39*, 221–229.
(9) Stoltz, B. M. *Chem. Lett.* **2004**, *33*, 362–367.
(10) ten Brink, G. J.; Arends, I. W. C. E.; Sheldon, R. A. *Science* **2000**, *287*, 1636–1639.
(11) Marko, I. E.; Giles, P. R.; Tsukazaki, M.; Brown, S. M.; Urch, C. J. *Science* **1996**, *274*, 2044–2046.
(12) Gamez, P.; Arends, I. W. C. E.; Sheldon, R. A.; Reedijk, J. *Adv. Synth. Catal.* **2004**, *346*, 805–811.
(13) Jiang, N.; Ragauskas, A. J. *J. Org. Chem.* **2006**, *71*, 7087–7090.
(14) Marko, I. E.; Gautier, A.; Dumeunier, R.; Doda, K.; Philippart, F.; Brown, S. M.; Urch, C. J. *Angew. Chem., Int. Ed.* **2004**, *43*, 1588–1591.
(15) Michel, C.; Belanzoni, P.; Gamez, P.; Reedijk, J.; Baerends, E. J. *Inorg. Chem.* **2009**, *48*, 11909–11920.
(16) Gamez, P.; Arends, I. W. C. E.; Reedijk, J.; Sheldon, R. A. *Chem. Commun.* **2003**, 2414–2415.
(17) Chaudhuri, P.; Hess, M.; Mueller, J.; Hildenbrand, K.; Bill, E.; Weyhermueller, T.; Wieghardt, K. *J. Am. Chem. Soc.* **1999**, *121*, 9599–9610.
(18) Chaudhuri, P.; Hess, M.; Florke, U.; Wieghardt, K. *Angew. Chem., Int. Ed.* **1998**, *37*, 2217–2220.

10.1021/ja105739k

Scheme 1. (a) Hydride-Transfer Step Proposed by Uemura and Co-workers for the Oxidation of Propargylic Alcohols[20] and (b) Oxidation of Cyclopropyl-Substituted α-Hydroxy Ester **A**, As Observed by Toste and Co-workers, Proceeds with No Ring Opening, Suggesting a Hydride-Transfer Pathway[24]

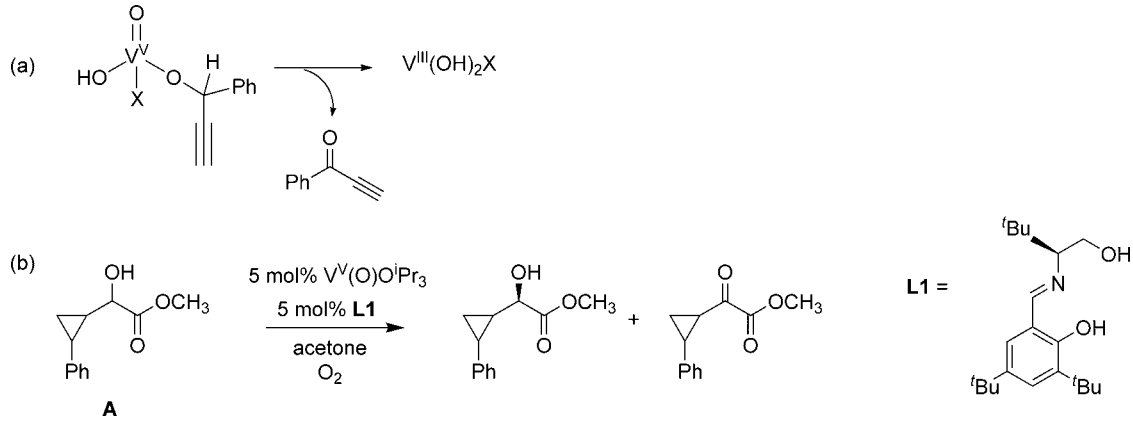

propargylic alcohols catalyzed by $V^{IV}(O)(acac)_2$.[19,20] The substrate scope of this reaction was subsequently extended by Ragauskas and co-workers, who found that the combination of $V^{IV}(O)(acac)_2$ and DABCO (DABCO = 1,4-diazabicyclo[2.2.2]-octane) catalyzed the aerobic oxidation of benzylic and allylic alcohols in ionic liquid solvent.[21,22] More recently, Ohde and Limberg have reported a metavanadate-cinnamic acid system which is also effective for the aerobic oxidation of activated alcohols.[23] Toste and Chen have developed processes for the aerobic oxidative kinetic resolution of α-hydroxyesters, α-hydroxyamides, and α-hydroxyphosphonates using chiral Schiff-base vanadium complexes.[24−26] At higher temperatures, Velusamy and Punniyamurthy have found that V_2O_5 catalyzes the aerobic oxidation of primary and secondary aliphatic alcohols in toluene solvent.[27]

Despite an increasing frequency of reports of metal-catalyzed aerobic oxidation, little is known about the mechanism of vanadium-mediated alcohol oxidation. Uemera and co-workers found that the radical inhibitors 2,6-di-*tert*-butyl-4-methylphenol (BHT) and galvinoxyl did not affect the catalytic oxidation of propargylic alcohols, and thus proposed that the reaction proceeds through a vanadium(III) intermediate formed via hydride transfer from the alkoxide ligand to the vanadium−oxo ligand (Scheme 1a).[19,20] A similar pathway for the oxidative kinetic resolution of α-hydroxyesters was proposed by Toste and co-workers, based on the finding that the cyclopropyl-substituted α-hydroxyester **A** was oxidized with no ring opening (Scheme 1b).[24] Chen and co-workers also favored a hydride-transfer pathway for the oxidative kinetic resolution of α-hydroxyesters, amides, and phosphonates, but no in-depth mechanistic study has been carried out on any of the catalytic systems.[25,26]

Although hydride-transfer pathways were proposed for the vanadium-catalyzed alcohol oxidations discussed above, one-electron pathways involving a vanadium(IV) intermediate have also frequently been invoked for vanadium mediated alcohol oxidation. The mechanism of the stoichiometric oxidation of alcohols by vanadate ($V^VO_2^+$) in aqueous acidic solution has been extensively studied, and is thought to proceed through radical intermediates.[28−31] Ohde and Limberg have proposed a hydrogen atom abstraction pathway for the oxidation of alcohols by a vanadium(V) cinnamate complex, based on a primary kinetic isotope effect and an observed correlation of the turnover frequency with homolytic C−H bond strength.[23] Given the variety of pathways proposed, a greater understanding of the mechanisms of vanadium-mediated alcohol oxidation could facilitate the development of more effective and versatile aerobic oxidation catalysts.

We report here the results of a detailed study of the mechanism of alcohol oxidation by dipicolinate vanadium(V). Our findings suggest that the alcohol oxidation reaction proceeds by an entirely different pathway than that proposed for palladium or copper complexes, and differs substantially from what has been proposed for other vanadium catalysts. Kinetic studies have elucidated the role of pyridine in the elementary oxidation step, and oxidation of two substrate probes suggests a two-electron pathway involving a vanadium(III) intermediate. Trends in reactivity based on varying substitution of the dipicolinate ligand and the pyridine base are established.

Results

Synthesis of Vanadium(V) Alkoxide Complexes. As previously reported,[32] the isopropoxide ligand on the complex (dipic)V^V(O)(O^iPr) (**1**) (dipic = dipicolinate) exchanges readily with free alcohol at room temperature, enabling the facile synthesis of a number of alkoxide derivatives. The *n*-butanoxide complex (dipic)V^V(O)(OBu) (**2**) was prepared by reaction of **1** with an excess of 1-butanol in acetonitrile solvent, followed by removal of the solvent under vacuum. The complexes (dipic)-V^V(O)(OCyBu) (**3**) (OCyBu = cyclobutanoxide) and (dipic)-V^V(O)(TBA) (**4**) (TBA = α-*tert*-butylbenzylalkoxide) were prepared from cyclobutanol and α-*tert*-butylbenzylalcohol using similar procedures (Figure 1, see experimental section for

(19) Maeda, Y.; Kakiuchi, N.; Matsumura, S.; Nishimura, T.; Uemura, S. *Tetrahedron Lett.* **2001**, *42*, 8877–8879.
(20) Maeda, Y.; Kakiuchi, N.; Matsumura, S.; Nishimura, T.; Kawamura, T.; Uemura, S. *J. Org. Chem.* **2002**, *67*, 6718–6724.
(21) Jiang, N.; Ragauskas, A. J. *Tetrahedron Lett.* **2006**, *48*, 273–276.
(22) Jiang, N.; Ragauskas, A. J. *J. Org. Chem.* **2007**, *72*, 7030–7033.
(23) Ohde, C.; Limberg, C. *Chem.—Eur. J.* **2010**, *16*, 6892–6899.
(24) Radosevich, A.; Musich, C.; Toste, F. D. *J. Am. Chem. Soc.* **2005**, *127*, 1090–1091.
(25) Pawar, V. D.; Bettigeri, S.; Weng, S. S.; Kao, J. Q.; Chen, C. T. *J. Am. Chem. Soc.* **2006**, *128*, 6308–6309.
(26) Weng, S. S.; Shen, M. W.; Kao, J. Q.; Munot, Y. S.; Chen, C. T. *Proc. Natl. Acad. Sci. U.S.A.* **2006**, *103*, 3522–3527.
(27) Velusamy, S.; Punniyamurthy, T. *Org. Lett.* **2004**, *6*, 217–219.
(28) West, D. M.; Skoog, D. A. *J. Am. Chem. Soc.* **1960**, *82*, 280–283.
(29) Littler, J. S.; Waters, W. A. *J. Chem. Soc.* **1959**, 1299–1305.
(30) Littler, J. S.; Waters, W. A. *J. Chem. Soc.* **1959**, 4046–4052.
(31) Littler, J. S.; Waters, W. A. *J. Chem. Soc.* **1960**, 2767–2772.
(32) Thorn, D. L.; Harlow, R. L.; Herron, N. *Inorg. Chem.* **1996**, *35*, 547–548.

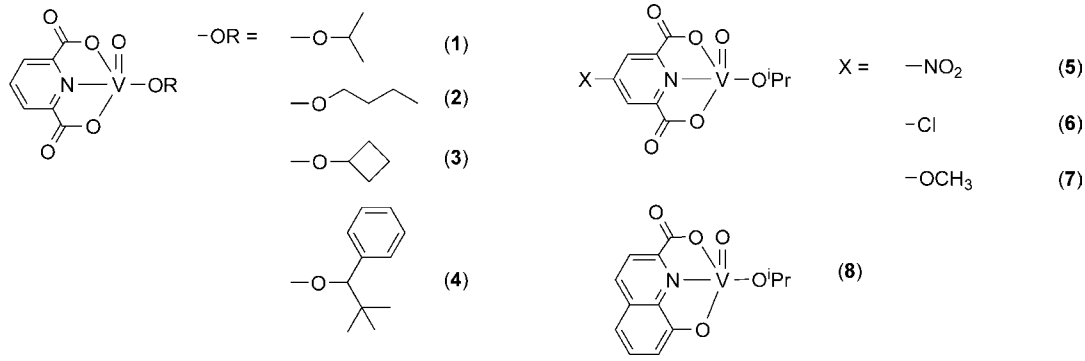

Figure 1. Vanadium(V) alkoxide complexes.

details). The dipicolinate alkoxide complexes generally co-crystallize with one equivalent of the alcohol. The ^{1}H NMR spectra of the dipicolinate complexes in CD_3CN show characteristic resonances for the V-OC*H* protons on the alkoxide ligand that are shifted significantly upfield from the corresponding resonance of the free alcohol, at 6.35 ppm for **1**, 5.99 ppm for **2**, 6.41 ppm for **3**, and 7.15 ppm for **4**. The IR spectra of **1**−**4** show sharp $\nu_{V=O}$ stretching frequencies in the range of 988−991 cm^{-1}.

Several additional vanadium(V) isopropoxide complexes were prepared using derivatives of dipicolinic acid. Reaction of 4-nitrodipicolinic acid (H_2dipicNO_2) or 4-chlorodipicolinic acid (H_2dipicCl) with $V^V(O)(O^iPr)_3$ in isopropanol afforded the complexes (dipicNO_2)$V^V(O)(O^iPr)$ (**5**) and (dipicCl)$V^V(O)(O^iPr)$ (**6**), respectively. 4-Methoxydipicolinic acid (H_2dipicOMe) was prepared using a published procedure,[33,34] and reaction with $V^V(O)(O^iPr)_3$ in isopropanol yielded (dipicOMe)$V^V(O)(O^iPr)$ (**7**). Finally, reaction of 8-hydroxyquinoline-2-carboxylic acid (H_2HQC) with $V^V(O)(O^iPr)_3$ in acetonitrile solvent yielded (HQC)$V^V(O)(O^iPr)$ (**8**). The ^{1}H NMR spectra of complexes **5**−**8** (CD_3CN) show resonances for the methine protons on the isopropoxide ligand that shift downfield as the electron-donating ability of the ligand increases, at 6.51 ppm for **5**, 6.39 ppm for **6**, 6.22 ppm for **7**, and 6.07 ppm for **8**. A single resonance is evident in the ^{51}V NMR spectra of complexes **5**−**8**, appearing at −588.2, −588.9, −590.3, and −549.8 ppm, respectively.

Coordination of Pyridine to 1. Addition of pyridine to a CD_3CN solution of **1** resulted in an immediate change in the ^{1}H NMR chemical shifts of **1**, suggestive of coordination of pyridine to **1**. The change in chemical shift was particularly pronounced for the methine resonance on the isopropoxide ligand of **1**, which shifted from 6.35 ppm to 6.50 ppm upon addition of 1 equiv pyridine. Titrating the sample with increasing amounts of pyridine revealed that the chemical shifts of both **1** and pyridine varied as a function of pyridine concentration. Sharp signals were observed for both pyridine and the isopropoxide complex at room temperature, consistent with a fast exchange process. A similar change in chemical shift as a function of pyridine was also noted for the ^{51}V NMR signal of **1** (Figure 2). In both the ^{1}H and ^{51}V NMR titration experiments, the change in chemical shift leveled off at concentrations of pyridine greater than ca. 0.6 M, indicating an equilibrium coordination of pyridine according to eq 1. Titrations were also

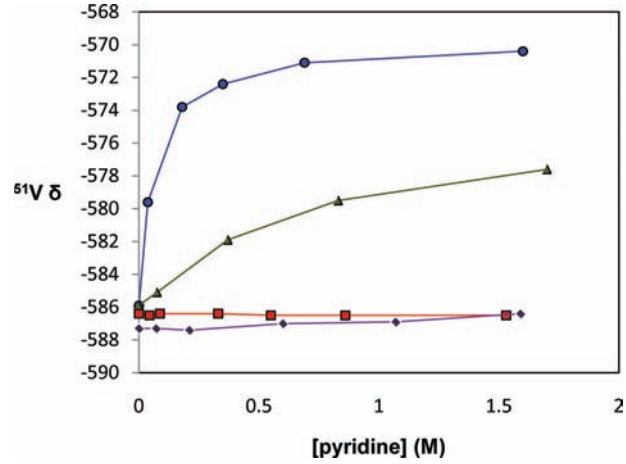

Figure 2. Plot of ^{51}V NMR chemical shift (CD_3CN) vs concentration of pyridine, 298 K (red squares, 2,6-di-*tert*-butylpyridine; purple diamonds, 2,6-lutidine; green triangles, 4-cyanopyridine; and blue circles, pyridine).

carried out with 4-cyanopyridine, 2,6-lutidine, and 2,6-di-*tert*-butylpyridine (Figure 2). 2,6-Di-*tert*-butypyridine and 2,6-lutidine are expected to be too sterically hindered to coordinate to the vanadium center and the chemical shifts of **1** were unaffected by the addition of either of these bulky bases, confirming that the change in chemical shift observed for the parent pyridine is due to pyridine coordination and not due to a medium effect or a change in solvent polarity. From the NMR data, values of K_{eq} of 15(±2) M^{-1} for pyridine and 2(±1) M^{-1} for 4-cyanopyridine at 298 K could be calculated (using the average of two independent titrations) according to eqs 2−3. For pyridine, a value of K_{eq} of 2(±1) M^{-1} was also determined at 340 K (the temperature at which kinetic studies of the pyridine dependence of the reaction were carried out, *vide infra*).

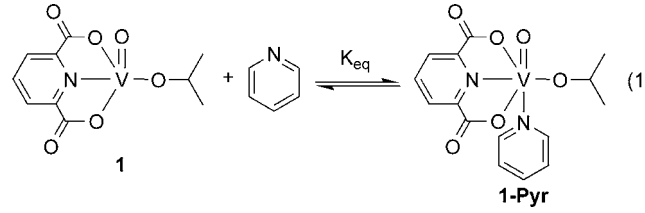

(1)

$$K_{eq} = \frac{[\mathbf{1\text{-}Pyr}]}{[\mathbf{1}][\mathrm{Pyr}]} \quad (2)$$

$$K_{eq} = \frac{\delta - \delta_1}{(\delta_{1Pyr} - \delta)[\mathrm{Pyr}]} \quad (3)$$

(33) Pellegatti, L.; Zhang, J.; Drahos, B.; Villette, S.; Suzenet, F.; Guillaumet, G.; Petoud, S.; Toth, E. *Chem. Commun.* **2008**, 6591–6593.
(34) Gassner, A. L.; Duhot, C.; Bunzli, J. C. G.; Chauvin, A. S. *Inorg. Chem.* **2008**, *47*, 7802–7812.

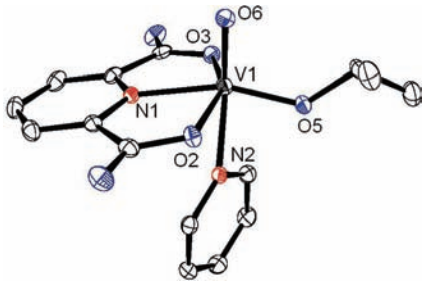

Figure 3. X-ray structure of **1-Pyr** (thermal ellipsoids shown at 50% probability, H atoms omitted for clarity). Selected bond lengths (Å) for **1-Pyr**: V1−O6 = 1.585(1), V1−O5 = 1.755(1), V1−O3 = 1.958(1), V1−O2 = 1.951(1), V1−N1 = 2.088(2), V1−N2 = 2.369(2).

The coordination of pyridine was confirmed by X-ray crystallography; yellow crystals of (dipic)V^{V}(O)(O^{i}Pr)(pyr) (**1-Pyr**) were obtained by diffusing diethyl ether into a pyridine solution of **1** at −20 °C. The pyridine ligand in **1-Pyr** is coordinated trans to the oxo ligand, and the distance between the vanadium center and the pyridine nitrogen is relatively long (2.369(2) Å) compared to that between the vanadium and the nitrogen of the dipic ligand (2.088(2) Å). The vanadium−oxo (1.585(1) Å) and vanadium−isopropoxide oxygen (1.755(1) Å) bond distances in **1-Pyr** are nearly identical to those of **1** (1.588(3), 1.756(3) Å).[32] Consistent with a fast exchange of free and bound pyridine, the equilibrium described in eqs 1 and 2 was established immediately upon dissolving isolated **1-Pyr** in CD_3CN.

Thermolysis of Vanadium(V) Alkoxide Complexes. Complexes **1** and **2** are stable for days in acetonitrile solution at room temperature. In the absence of base, **1** and **2** reacted very slowly at elevated temperatures. For instance, when a solution of **1** in CD_3CN was heated at 100 °C for 3 weeks, less than 25% of the starting material reacted, as judged by integration against an internal standard. However, complex **1** reacted cleanly with pyridine in CD_3CN solution over several days at room temperature (or 30 min at 100 °C) to afford acetone (0.5 equiv, 100% yield), isopropanol (0.5 equiv, 100% yield), and the vanadium(IV) complex (dipic)V^{IV}(O)(pyr)$_2$ (**9**), according to eq 4 (yields expressed as a percentage of the theoretical maximum based on the oxidizing equivalents of vanadium consumed). The butanoxide complex **2** reacted in pyr-d_5 solution over 30 min at 100 °C to afford butyraldehyde (80%) and **9**. Complex **9** has been previously described and was characterized by IR, ^{1}H NMR, and UV−vis spectroscopy and X-ray crystallography.[35]

To gain insight into the mechanism of alcohol oxidation, the oxidation of mechanistic probes cyclobutanol and α-*tert*-butylbenzylalcohol was studied. Cyclobutanoxide complex

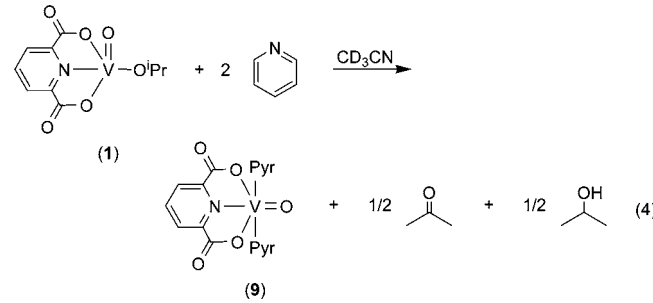

3 reacted in pyr-d_5 solution over 30 min at 100 °C to afford cyclobutanone (93% yield) and **9** (Scheme 2). No ring-opened products were detected by ^{1}H NMR spectroscopy. Thermolysis of complex **4** in pyr-d_5 solution (20 min at 100 °C) afforded the ketone 2,2-dimethylpropiophenone (98% yield) and **9** (Scheme 2). No C−C bond fission products (such as benzaldehyde) were formed in this reaction. In contrast, in the absence of pyridine in CD_3CN solution, complex **4** reacted more slowly (2 weeks at room temperature), affording benzaldehyde (92% yield) as the major organic product.[36] The fate of the *tert*-butyl moiety in this reaction is still under investigation;[37] however, the formation of benzaldehyde is suggestive of radical intermediates. To test for the possible involvement of radicals, the reactivity of **4** was studied in the presence of 9,10-dihydroanthracene. In the reaction of **4** in pyr-d_5 solvent, no change in reaction products or yield and no formation of anthracene was detected by ^{1}H NMR spectroscopy. However, when 9,10-dihydroanthracene (4 equiv) was added to the reaction of **4** in CD_3CN, the formation of anthracene (12% yield, based on the oxidizing equivalents of vanadium consumed) was observed by ^{1}H NMR spectroscopy.

The 8-quinolinate-2-carboxylate (HQC) complex **8** reacted in pyr-d_5 solvent over 2.5 h at 100 °C to afford acetone (0.5 equiv, 90% yield) and the new vanadium(IV) complex (HQC)-V^{IV}(O)(pyr)$_2$ (**10**). Complex **10** was characterized by elemental analysis, as well as UV−vis and IR spectroscopy ($\nu_{V=O}$ = 957 cm^{-1}). The orientation of the oxo ligand in **10** with respect to the HQC ligand is unclear, as several crystals of **10** grown from pyridine solution were found to be disordered. Complex **10** was recrystallized from DMSO, yielding the complex (HQC)-V^{IV}(O)(DMSO)$_2$ (**11**). Complex **11** showed a vanadium−oxo stretch in the IR spectrum at $\nu_{V=O}$ = 950 cm^{-1}, and X-ray diffraction (Figure 4) revealed that the oxo ligand is trans to a DMSO ligand, in contrast to the related complex (dipic)-V^{IV}(O)(DMSO)$_2$.[38]

Scheme 2. Oxidation of Cyclobutanol and α-*tert*-Butylbenzyl Alcohol

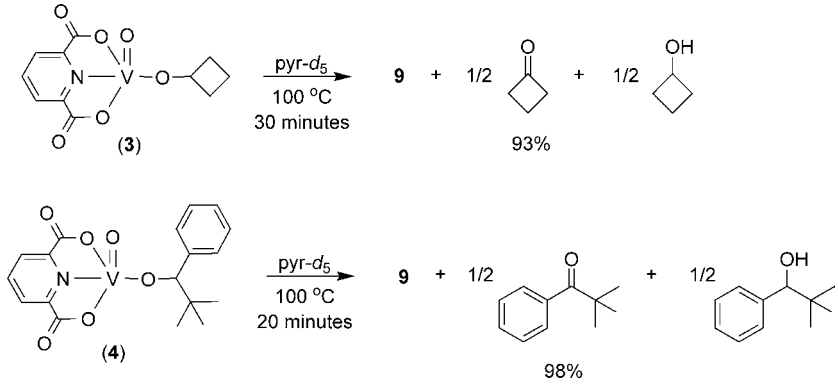

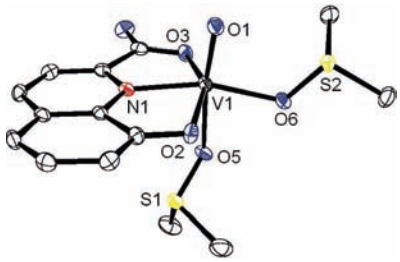

Figure 4. X-ray structure of **11** (thermal ellipsoids shown at 50% probability, H atoms omitted for clarity). Selected bond lengths (Å) for **11**: V1−O1 = 1.603(2), V1−N1 = 2.011(2), V1−O2 = 2.033(2), V1−O6 = 2.048(2), V1−O3 = 2.070(2), V1−O5 = 2.198(2).

The dipicOMe complex **7** reacted in pyr-d_5 solution (30 min at 100 °C) to afford acetone (0.5 equiv, 98% yield) and (dipicOMe)V^{IV}(O)(pyr)$_2$ (**12**). Complex **12** was characterized by X-ray crystallography, UV−vis and IR spectroscopy, and elemental analysis. The V═O stretching frequency of 960 cm^{-1} is slightly lower than that of the parent dipic complex **9** (965 cm^{-1}), and the X-ray structure of **12** (Figure S1, Supporting Information) indicates that the oxo ligand is trans to the nitrogen of the dipic ligand. The dipicCl complex **6** also reacted in pyr-d_5 solvent (30 min at 100 °C), yielding acetone (0.5 equiv, 100% yield) and a green-brown precipitate. The precipitate showed a V═O stretch in the IR at 962 cm^{-1}, consistent with (dipicCl)V^{IV}(O)(pyr)$_2$ (**13**).[39]

Unlike the other complexes, dipicNO_2 complex **5** did not react cleanly in pyridine solution to form vanadium(IV) and acetone. Complex **5** co-crystallized with water and reacted in pyridine solution to generate the *cis*-dioxo complex [(dipicNO_2)-V^{V}(O)$_2$]HPyr (**14**). Repeated attempts to obtain complex **5** free of water by recrystallization of **5** from isopropanol or by pre-drying the dipicNO_2 ligand under high vacuum (48 h) or over molecular sieves were unsuccessful. Complex **14** was isolated in 52% yield, and ^{1}H and ^{51}V NMR spectra were consistent with those reported by Crans and co-workers for the *cis*-dioxo complex [(dipicNO_2)V^{V}(O)$_2$]K.[40]

Conproportionation of V^{III}/V^{V}. The reactions of the dipic vanadium(V) complexes described above produce vanadium(IV) and 0.5 equiv of a two-electron-oxidized organic product. One possible pathway for this reaction would be an initial two-electron oxidation of the alkoxide ligand of the vanadium(V) complex, forming a vanadium(III) intermediate. A subsequent fast conproportionation reaction between vanadium(V) and vanadium(III) would result in the formation of the vanadium(IV) product. This type of V^{V}/V^{III} conproportionation reaction was tested. A pyridine solution of [(dipic)V^{V}(O)$_2$]HPyr (**15**) was treated with 0.5 equiv of the dimer [(dipic)V^{III}(pyr)$_2$]$_2$(μ-O) (**16**).[35] Within seconds of mixing the two complexes in pyridine solution, the intense purple color of the V^{III} dimer faded and the solution turned a green color. UV−vis and IR spectra of the reaction mixture were consistent with quantitative formation of (dipic)V^{IV}(O)(pyr)$_2$ (**9**) (eq 5).

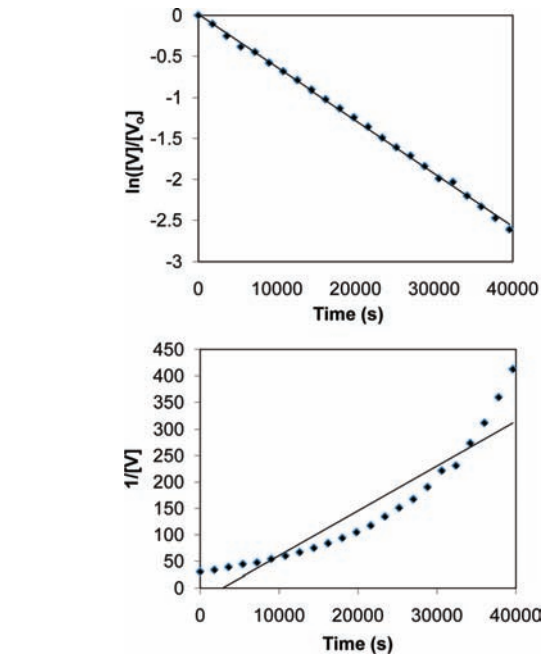

Figure 5. Kinetic plots of the thermolysis of **1** in pyr-d_5 solvent (319 K): top, fit to integrated first-order rate law; bottom, fit to integrated second-order rate law.

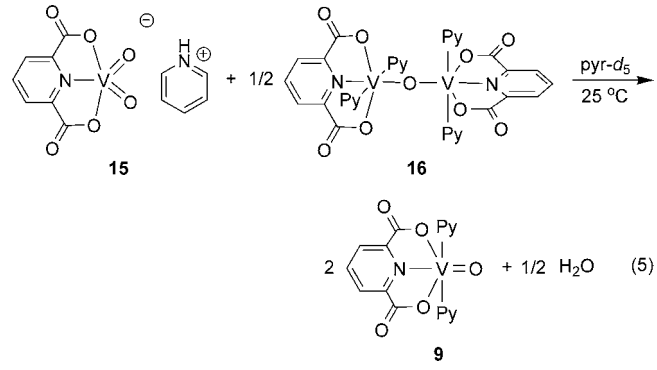

(5)

Kinetic Studies of Isopropanol Oxidation: Determination of Reaction Order. The reaction of **1** in pyridine-d_5 solvent to form acetone and **9** was monitored by ^{1}H NMR spectroscopy. Fitting the disappearance of **1** to the integrated first- and second-order rate laws indicated that the reaction is first-order in vanadium through at least three half-lives (Figure 5). In pyridine-d_5 solvent at 319 K, the observed first-order rate constant was k_{obs} = 7.0(5) × 10^{-5} s^{-1} for the rate law d[V_t]/dt = −k_{obs}[V_t], where [V_t] is the total concentration of compounds **1** and **1-Pyr**. When the reaction was carried out in the presence of the potential radical trap 9,10-dihydroanthracene (0.06 M), the reaction products and rate were unaffected (k_{obs} = 6.8(5) × 10^{-5} s^{-1}). The thermolysis of **1** in pyridine-d_5 solvent was also monitored by ^{51}V NMR spectroscopy. The first-order disap-

(35) Hanson, S. K.; Baker, R. T.; Gordon, J. C.; Scott, B. L.; Sutton, A. D.; Thorn, D. L. *J. Am. Chem. Soc.* **2009**, *131*, 428–429.
(36) The vanadium product of this reaction was a pale green precipitate, formulated as (dipic)V^{IV}(O)(CD_3CN)$_x$. Dissolution of this material in pyridine formed the known compound (dipic)V^{IV}(O)(pyr)$_2$.
(37) *tert*-Butanol was detected by ^{1}H NMR in approximately 70% yield, along with several other minor unidentified products.
(38) Hanson, S. K.; Baker, R. T.; Gordon, J. C.; Scott, B. L.; Thorn, D. L. *Inorg. Chem.* **2010**, *49*, 5611–5618.
(39) The related complex (dipicCl)V^{IV}(O)(H_2O)$_2$ has been reported: Smee, J. J.; Epps, J. A.; Ooms, K.; Bolte, S. E.; Polenova, T.; Baruah, B.; Yang, L.; Ding, W.; Li, M.; Willsky, G. R.; la Cour, A.; Anderson, O. P.; Crans, D. C. *J. Inorg. Biochem.* **2009**, *103*, 575–584.
(40) Smee, J. J.; Epps, J. A.; Teissedre, G.; Maes, M.; Harding, N.; Yang, L.; Baruah, B.; Miller, S. M.; Anderson, O. P.; Willsky, G. R.; Crans, D. C. *Inorg. Chem.* **2007**, *46*, 9827–9840.

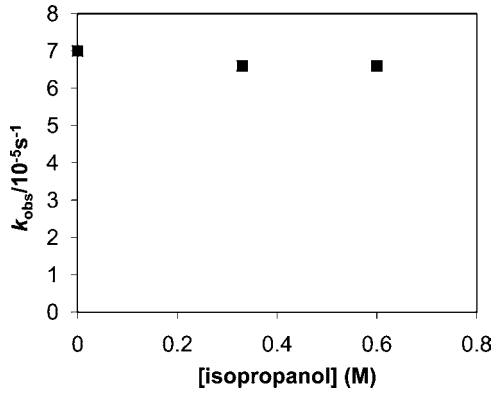

Figure 6. Observed rate constants for the reaction of **1** at 319 K in pyr-d_5 with varying concentrations of isopropanol.

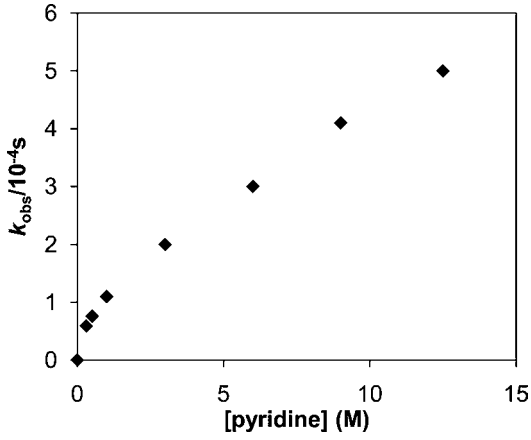

Figure 7. Observed rate constants for the reaction of **1** in mixtures of CD_3CN and pyr-d_5, 340 K.

pearance of **1** was observed, with no intermediates or other species detected during the reaction.[41]

The concentration of added isopropanol was varied from 0 to 0.6 M (319 K), and no change in the reaction rate was observed, indicating a zero-order dependence on isopropanol (Figure 6). In contrast, the dependence of the reaction rate on the concentration of pyridine was more complex (Figure 7). At 340 K, the reaction of **1** was carried out in mixtures of CD_3CN and pyr-d_5 solvents, over a pyridine concentration range of 0−12.5 M. At higher concentrations of pyr-d_5 (3−12.5 M), k_{obs} exhibited a linear dependence on pyridine concentration. A line fit to the data for k_{obs} vs [pyridine] for pyridine concentrations of 3−12.5 M gave a slope of 3.2×10^{-5} and a positive y-intercept of 1.1×10^{-4} ($r^2 = 0.995$). Deviation from this linear dependence was observed at low concentrations of pyridine, with the reaction rate approaching zero as the concentration of pyridine approaches zero.

Measuring the reaction rate in pyr-d_5 solvent at five temperatures between 319 and 360 K yielded activation parameters of $\Delta H^{\ddagger} = 20(2)$ kcal/mol (85(4) kJ/mol) and $\Delta S^{\ddagger} = -14(1)$ eu (−57(6) J/mol·K) (Figure 8, Table 1). Finally, the deuterated isopropoxide complex **1-*d*$_7$** was prepared from the reaction of **1** with isopropanol-d_8. Comparison of the reaction rates of **1** and **1-*d*$_7$** in pyr-d_5 solvent allowed for determination of a primary kinetic isotope effect of $k_H/k_D = 5.7(5)$ at 340 K.

(41) See Supporting Information for representative ^{51}V NMR spectra from the reaction.

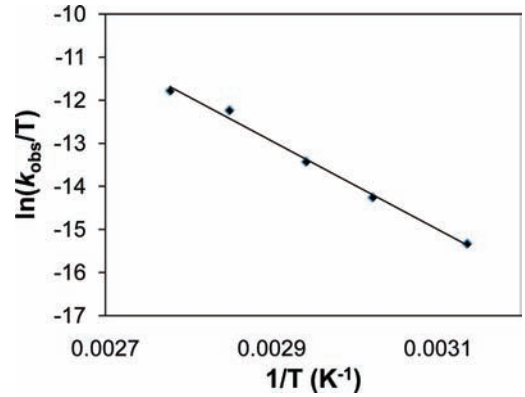

Figure 8. Eyring plot for the reaction of **1** in pyridine-d_5 solvent, 319−360 K.

Table 1. Values of k_{obs} for the Reaction of **1** in Pyr-d_5 Solvent, 319−360 K

temp (K)	k_{obs} (s^{-1})
319	$7.0(5) \times 10^{-5}$
331	$2.1(1) \times 10^{-4}$
340	$5.0(3) \times 10^{-4}$
351	$1.7(1) \times 10^{-3}$
360	$2.5(2) \times 10^{-3}$

Table 2. Values of pK_a, σ, and k_{bimol} for the Reactions of 4-Substituted Pyridines with **1** (CD_3CN, 340 K)

R	pK_a ($[H(R\text{-}Pyr)]^+$)[44,45]	σ[42,43]	k_{bimol} (M^{-1} s^{-1})
$-OCH_3$	6.47	−0.27	$7.6(6) \times 10^{-4}$
$-CH_3$	6.03	−0.17	$3.0(4) \times 10^{-4}$
−H	5.25	0	$1.1(3) \times 10^{-4}$
$-CF_3$	2.63	0.55	$5.3(6) \times 10^{-6}$
−CN	1.90	0.63	$4.1(4) \times 10^{-6}$

Reaction of (dipic)V(O)O^{i}Pr with Substituted Pyridines. In CD_3CN solution, the reaction of complex **1** was studied with a number of different *para*-substituted pyridines at 340 K. A greater than 10-fold excess concentration of the pyridine was used to ensure pseudo-first-order kinetic behavior. For 4-cyanopyridine and 4-trifluoromethylpyridine, the reactions were carried out at pyridine concentrations of greater than 0.8 M. For pyridine, 4-methylpyridine (4-picoline), and 4-methoxypyridine, reactions were carried out at pyridine concentrations of greater than 0.5 M. Approximate second-order rate constants k_{bimol} were calculated by dividing k_{obs} by the concentration of pyridine (Table 2). The reaction rate showed a significant dependence on the pyridine substituent, with 4-methoxypyridine reacting with **1** more than 200 times faster ($k_{bimol} = 7.6(6) \times 10^{-4}$ $M^{-1}s^{-1}$) than 4-cyanopyridine ($k_{bimol} = 4.1(4) \times 10^{-6}$ $M^{-1}s^{-1}$). The data fit well to a Hammett plot, giving slope $\rho = -2.5$ ($r^2 = 0.995$) (Figure 9).[42,43] The log of the bimolecular rate constant also correlates well with the pK_a of the pyridine,[44,45] giving a linear plot ($r^2 = 0.985$) (Figure 10).

The reaction of **1** was also studied with 2,6-lutidine (0.5 M) in CD_3CN at 340 K. Acetone was produced in 67% yield, but a side reaction occurred that was not observed for any of the

(42) Jaffe, H. H. *Chem. Rev.* **1953**, *53*, 191–261.
(43) Exner, O. In *Advances in Linear Free Energy Relationships*; Chapman, N. B., Shorter, J., Eds.; Plenum Press: London, 1972; pp 2−52.
(44) Mason, S. F. *J. Chem. Soc.* **1959**, 1247–1253.
(45) Taagepera, M.; Henderson, W. G.; Brownlee, R. T. C.; Beauchamp, J. L.; Holtz, D.; Taft, R. W. *J. Am. Chem. Soc.* **1972**, *94*, 1369–1370.

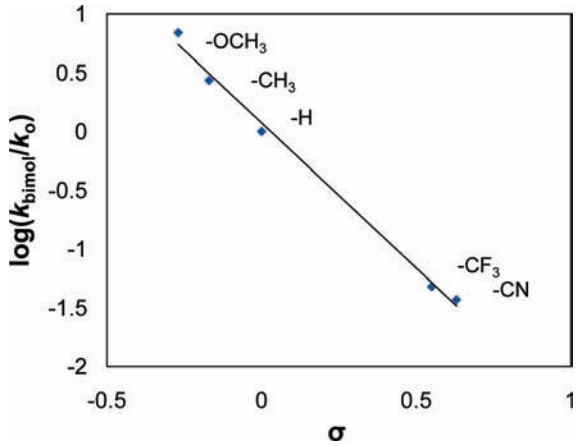

Figure 9. Hammett plot for the reaction of **1** with *para*-substituted pyridines in CD_3CN solvent, 340 K.

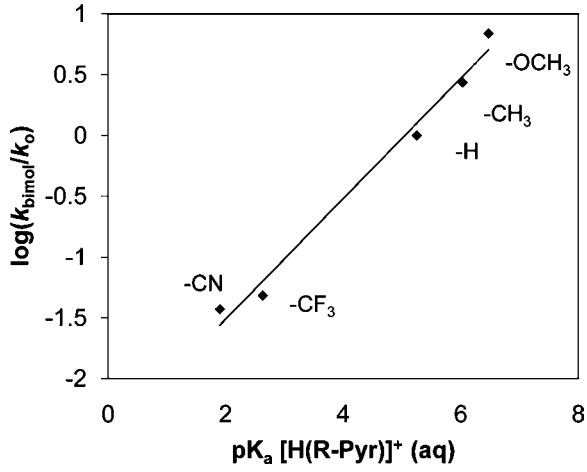

Figure 10. Plot of pK_a $[H(R\text{-}Pyr)]^+$ versus $\log(k_{bimol}/k_o)$ for the reactions of 4-substituted pyridines.

unhindered pyridines. As the reaction progressed, the vanadium(V) complex $V^V(O)(O^iPr)_3$ was formed, reaching a maximum of ~28% yield at 80% conversion. The formation of $V^V(O)(O^iPr)_3$ likely results from the removal of the dipicolinate ligand from **1** in the presence of 2,6-lutidine and isopropanol, which is formed as the reaction progresses.[46] The lack of formation of $V^V(O)(O^iPr)_3$ in the reaction of **1** with the unhindered pyridines may reflect the stabilization of complex **1** via pyridine coordination, which does not occur for the bulky 2,6-lutidine. In a separate experiment, thermolysis of $V^V(O)(O^iPr)_3$ with pyridine (3 equiv) in CD_3CN solution yielded less than 5% acetone after 3 weeks of heating at 100 °C, suggesting that formation of $V^V(O)(O^iPr)_3$ is not involved in the isopropanol oxidation pathway.

Effect of the Ligand on the Rate of Stoichiometric Isopropanol Oxidation. The reactions of vanadium(V) isopropoxide complexes **6**−**8** in pyr-d_5 solvent were monitored by ^1H NMR spectroscopy. At 340 K, the dipicOMe complex **7** reacted more slowly ($k_{obs} = 3.3(6) \times 10^{-4}$ s^{-1}) than the parent dipic complex **1** ($k_{obs} = 5.0(3) \times 10^{-4}$ s^{-1}). Replacing one of the carboxylate groups on the dipic ligand with a more electron-donating phenolate group in the 8-quinolinate-2-carboxylate complex **8** resulted in a significant reduction in reaction rate ($k_{obs} = 2.1(2) \times 10^{-5}$ s^{-1}). Determination of the rate constant for the reaction of the dipicCl complex **6** was complicated by precipitation of the vanadium(IV) product, which interfered with integration of the ^1H NMR spectrum at late reaction times. However, it was possible to obtain an estimate of $k_{obs} \approx 1.4 \times 10^{-3}$ s^{-1} using initial rate values, indicating that complex **6** reacts faster than **1** in pyr-d_5 solvent. The reaction rate of dipicNO_2 complex **5** was not measured due to the reaction with water noted above, forming the *cis*-dioxo complex **14**.

Table 3. Values of k_{obs} for Complexes **1** and **6**−**8** in pyr-d_5 Solvent, 340 K

complex	k_{obs} (s^{-1})
6	$\sim 1.4 \times 10^{-3}$
1	$5.0(3) \times 10^{-4}$
7	$3.3(6) \times 10^{-4}$
8	$2.1(2) \times 10^{-5}$

Discussion

Vanadium complexes are effective catalysts for a variety of oxidations, including the aerobic oxidation of activated alcohols,[21−23] the oxidative kinetic resolution of α-hydroxyesters, α-hydroxyamides, and α-hydroxyphosphonates,[24−26] the oxidative C−C bond cleavage of diols and α-hydroxyketones,[28,47−49] the stereoselective oxidative coupling of naphthols,[50,51] and the oxidative decarboxylation of 2- and 3-hydroxycarboxylic acids.[52−54] Vanadium alkoxide complexes are putative intermediates in nearly all of these transformations, and thus there is considerable interest in their reactivity.[55]

A one-electron pathway involving a vanadium(IV) intermediate has often been proposed for vanadium-mediated oxidations. For example, Littler and Waters have carried out detailed studies of the stoichiometric oxidation of alcohols by vanadate ($V^VO_2^+$) in acidic aqueous solution and proposed a mechanism wherein a vanadium(V) alkoxide complex reacts to generate vanadium(IV) and an organic radical, followed by a fast reaction of the radical with a second equivalent of vanadium(V).[28−31] Radical intermediates have also been invoked in the oxidative decarboxylation of 2- and 3-hydroxycarboxylic acids,[52−54] the oxidative cleavage of α-hydroxyketones and glycols,[28,47−49] and a recently reported C−O bond cleavage reaction in lignin model compounds.[56]

In contrast, a two-electron pathway involving a vanadium(III) intermediate is thought to be operative in several catalytic alcohol oxidation reactions. Hydride transfer from an alkoxide ligand to a vanadium−oxo ligand was postulated as a key step in the oxidative kinetic resolution of α-hydroxyesters, α-hy-

(46) Removal of the dipicolinate ligand from vanadium under basic conditions has been reported previously. Crans and co-workers found that in aqueous solution $[(dipic)V^V(O)_2]^-$ undergoes hydrolysis at pH >6.5 to form vanadate and $dipic^{2-}$. See ref 57.

(47) Littler, J. S.; Mallet, A. I.; Waters, W. A. *J. Chem. Soc.* **1960**, 2761–2766.
(48) Mehrotra, R. N. *J. Chem. Soc. B* **1968**, 1123–1127.
(49) Kirihara, M.; Takizawa, S.; Momose, T. *J. Chem. Soc., Perkin Trans. 1* **1998**, 7–8.
(50) Barhate, N. B.; Chen, C. T. *Org. Lett.* **2002**, *4*, 2529–2532.
(51) Takizawa, S.; Katayama, T.; Kameyama, C.; Onitsuka, K.; Suzuki, T.; Yanagida, T.; Kawai, T.; Sasai, H. *Chem. Commun.* **2008**, 1810–1812.
(52) Jones, J. R.; Waters, W. A.; Littler, J. A. *J. Chem. Soc.* **1961**, 630–633.
(53) Meier, I. K.; Schwartz, J. *J. Am. Chem. Soc.* **1989**, *111*, 3069–3070.
(54) West, D. M.; Skoog, D. A. *Anal. Chem.* **1959**, *31*, 583–586.
(55) Crans, D. C.; Chen, H.; Felty, R. A. *J. Am. Chem. Soc.* **1992**, *114*, 4543–4550.
(56) Son, S.; Toste, F. D. *Angew. Chem., Int. Ed.* **2010**, *49*, 3791–3794.

droxyamides, and α-hydroxyphosphonates, as well as the catalytic oxidation of propargylic alcohols.[20,24−26] A greater understanding of when one- and two-electron oxidations take place may provide opportunities for the development of more effective vanadium oxidation catalysts.

Dipicolinate vanadium complexes have been studied extensively in aqueous solution as insulin-mimetic compounds.[39,40,57−60] Under non-aqueous conditions, dipicolinate vanadium(V) complexes oxidize alcohols and have also been found to catalyze the aerobic oxidation of lignin model compounds.[38] The kinetic studies presented above, together with the results of the oxidation of substrate probes, strongly suggest the involvement of pyridine in alcohol oxidation by dipicolinate vanadium(V) complexes. Several possible mechanisms for this reaction are considered, as discussed below.

Oxidation of Mechanistic Probes. Roček, Lee, Bakac, Whitesides, and others have studied the oxidation of cyclobutanol to distinguish between one- and two-electron oxidations for a wide range of metals, including chromium, vanadium, copper, iron, and cerium.[61−69] The formation of cyclobutanone indicates a two-electron oxidation, whereas formation of ring-opened products such as 4-hydroxybutyraldehyde, butyraldehyde and crotonaldehyde (3-butene-1-al, from radical disproportionation), or suberaldehyde (1,8-octanedial, from radical dimerization) indicates a one-electron oxidation pathway.[61] The high yield of cyclobutanone (93%) observed in the reaction of dipicolinate vanadium complex **3** in pyr-d_5 solvent is consistent with a two-electron pathway involving a vanadium(III) intermediate. The lack of ring-opened products in this reaction resembles Toste's finding that the cyclopropyl-substituted α-hydroxyester **A** was oxidized by a vanadium(V) complex of a Schiff-base ligand with no ring opening (Scheme 1b).[24] In contrast, Roček found that vanadate ($V^VO_2^+$) oxidized cyclobutanol by a one-electron pathway, forming 4-hydroxybutyraldehyde in 94% yield.[63]

Kim, Nam, and co-workers have studied the oxidation of cyclobutanol by non-heme oxo iron(IV) complexes and proposed that formation of cyclobutanone results from an initial hydrogen atom transfer, followed by a fast electron transfer, giving a net hydride transfer and an iron(II) intermediate.[64] A similar pathway is possible for the dipicolinate vanadium system; the observation of no ring-opened products strongly suggests that a radical derived from cyclobutanol does not diffuse away from the vanadium center during the reaction.[64]

α-*tert*-Butylbenzyl alcohol (*tert*-butylphenylcarbinol) and its 4-methoxy-substituted derivative have been used by Westheimer, Waters, Baciocchi, Mayer, and others in mechanistic studies of metal-mediated oxidations.[70−75] Baciocchi and co-workers determined that one-electron oxidation of α-*tert*-butyl-4-methoxybenzyl alcohol generates a radical that undergoes rapid C−C bond fission, providing a way to distinguish pathways that proceed by hydride transfer or hydrogen atom transfer from those proceeding by initial electron transfer.[73] Thus, formation of the ketone product indicates a hydride-transfer or hydrogen-atom-transfer pathway, while formation of C−C bond fission products (benzaldehyde) indicates a pathway that proceeds by initial electron transfer.[73] In the reaction of dipicolinate complex **4** in pyr-d_5 solvent, the formation of 2,2-dimethylpropiophenone (98%) is consistent with a hydride-transfer or hydrogen-atom-abstraction pathway. Unlike complexes **1** and **2**, which show no reaction in the absence of pyridine, complex **4** reacts in CD_3CN solution (albeit slowly), affording benzaldehyde (92%) as the major product. Both the benzaldehyde product and the formation of anthracene observed when 9,10-dihydroanthracene is added to this reaction are consistent with radical intermediates. The fact that different products are formed in the oxidation of α-*tert*-butylbenzyl alcohol in the absence and in the presence of pyridine suggests that the pyridine is involved in the formation of the ketone product, enabling the two-electron pathway to dominate over a much slower one-electron pathway.

Mechanistic analysis based on interpretation of the reactivity of substrate probes can be complicated, due to the fact that the probe can, in some cases, react by a different pathway than other substrates. For example, Scott and Espenson found that cyclobutanol reacts with CrO^{2+} by a one-electron pathway, while other aliphatic alcohols react by a two-electron pathway.[76] This mechanistic change was attributed to the greater energetic expense of generating alkyl radicals from simple primary and secondary alcohols, as well as the greater stability of the simple aldehyde and ketone products as compared to the strained cyclobutanone.[76] Nevertheless, there are no known examples where a one-electron oxidant reacts with cyclobutanol to afford cyclobutanone as the product.[65] Furthermore, for the dipicolinate vanadium complexes, the results of the pyridine-promoted oxidation of cyclobutanol and α-*tert*-butylbenzyl alcohol are consistent. Taken together, the reactions of the mechanistic probes are strong evidence in support of a base-promoted two-electron pathway for the dipicolinate vanadium(V) oxidation that proceeds through a vanadium(III) intermediate.

Mechanism of Isopropanol Oxidation by 1. The dipicolinate vanadium(V) isopropoxide complex **1** reacts cleanly with pyridine to form the vanadium(IV) complex **9** and 0.5 equiv of acetone. No reaction of **1** is observed in the absence of pyridine, suggesting a key role for the base in the stoichiometric isopropanol oxidation.

(57) Crans, D. C.; Yang, L.; Jakusch, T.; Kiss, T. *Inorg. Chem.* **2000**, *39*, 4409–4416.
(58) Li, M.; Smee, J. J.; Ding, W.; Crans, D. C. *J. Inorg. Biochem.* **2009**, *103*, 585–589.
(59) Buglyo, P.; Crans, D. C.; Nagy, E. M.; Lindo, R. L.; Yang, L.; Smee, J. J.; Jin, W.; Chi, L. H.; Godzala, M. E., III; Willsky, G. R. *Inorg. Chem.* **2005**, *44*, 5416–5427.
(60) Crans, D. C.; Yang, L.; Alfano, J. A.; Chi, L. H.; Jin, W.; Mahroof-Tahir, M.; Robbins, K.; Toloue, M. M.; Chan, L. K.; Plante, A. J.; Grayson, R. Z.; Willsky, G. R. *Coord. Chem. Rev.* **2003**, *237*, 13–22.
(61) Meyer, K.; Rocek, J. *J. Am. Chem. Soc.* **1972**, *94*, 1209–1214.
(62) Rocek, J.; Radkowsky, A. E. *J. Am. Chem. Soc.* **1973**, *95*, 7123–7132.
(63) Rocek, J.; Aylward, D. E. *J. Am. Chem. Soc.* **1975**, *97*, 5452–5456.
(64) Oh, N. Y.; Suh, Y.; Park, M. J.; Seo, M. S.; Kim, J.; Nam, W. *Angew. Chem., Int. Ed.* **2005**, *44*, 4235–4239.
(65) Pestovsky, O.; Bakac, A. *J. Am. Chem. Soc.* **2004**, *126*, 13757–13764.
(66) Chandler, W. D.; Wang, Z.; Lee, D. G. *Can. J. Chem.* **2005**, *83*, 1212–1221.
(67) Lee, D. G.; Chen, T. *J. Org. Chem.* **1991**, *56*, 5341–5345.
(68) Coleman, K. S.; Lorber, C. Y.; Osborn, J. A. *Eur. J. Inorg. Chem.* **1998**, 1673–1675.
(69) Whitesides, G. M.; Sadowski, J. S.; Lilburn, J. *J. Am. Chem. Soc.* **1974**, *96*, 2829–2835.
(70) Hampton, J.; Leo, A.; Westheimer, F. H. *J. Am. Chem. Soc.* **1956**, *78*, 306–312.
(71) Jones, J. R.; Waters, W. A. *J. Chem. Soc.* **1960**, 2772–2773.
(72) Baciocchi, E.; Bietti, M.; Lanzalunga, O. *Acc. Chem. Res.* **2000**, *33*, 243–251.
(73) Baciocchi, E.; Bietti, M.; Putignani, L.; Steenken, S. *J. Am. Chem. Soc.* **1996**, *118*, 5952–5960.
(74) Bryant, J. M.; Taves, J. E.; Mayer, J. M. *Inorg. Chem.* **2002**, *41*, 2769–2776.
(75) Shearer, J.; Zhang, C. X.; Zakharov, L. N.; Rheingold, A. L.; Karlin, K. D. *J. Am. Chem. Soc.* **2005**, *127*, 5469–5483.
(76) Scott, S. L.; Bakac, A.; Espenson, J. H. *J. Am. Chem. Soc.* **1992**, *114*, 4205–4213.

Scheme 3. Possible Mechanisms for the Reaction of **1**

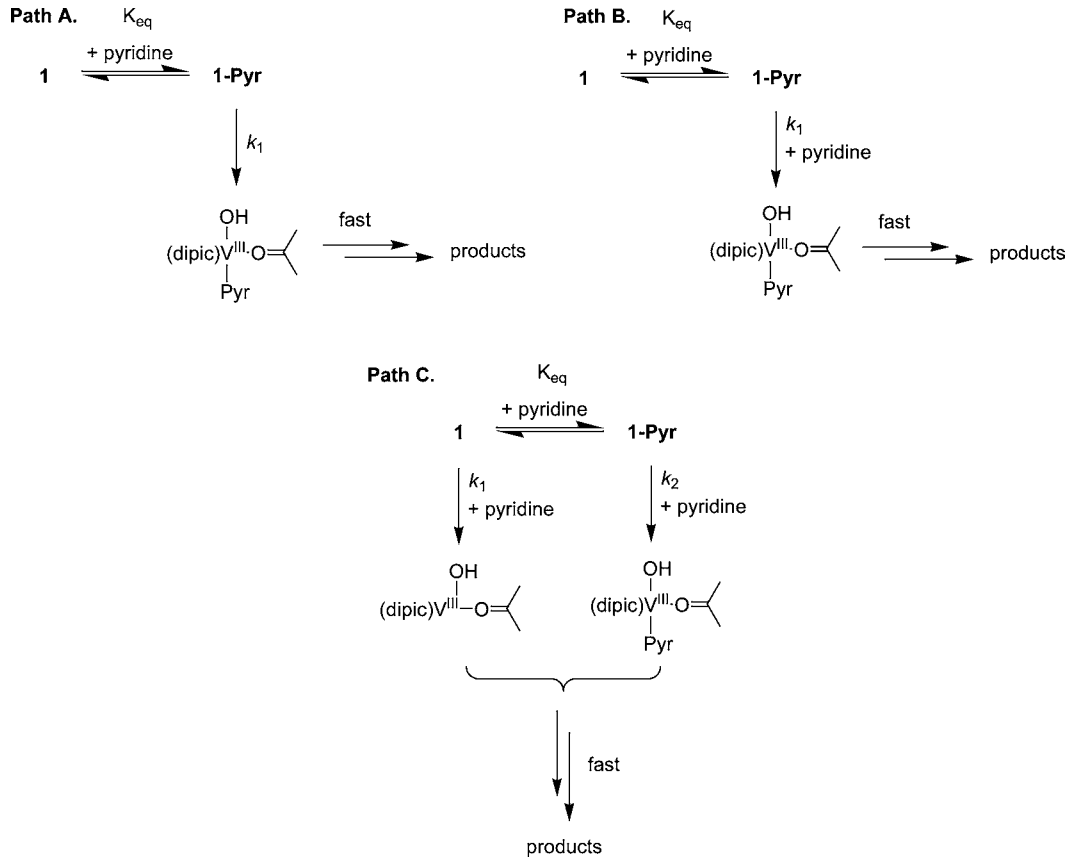

Three possible pathways for the reaction of **1** are shown in Scheme 3. All three pathways involve the coordination of pyridine to **1**, which is evident from the NMR titration experiments and the X-ray structure of **1-Pyr**. In each case, the slow step of the reaction is unimolecular in vanadium and involves breaking the C−H bond to generate a vanadium(III) intermediate, which is implicated by the primary kinetic isotope effect ($k_H/k_D = 5.7(5)$). A subsequent fast conproportionation of V^{III} and V^{V} would form the observed products. Conproportionation of the vanadium(V) complex $[(dipic)V^{V}(O)_2]HPyr$ (**15**) and the vanadium(III) complex $[(dipic)V^{III}(pyr)_2]_2(\mu\text{-}O)$ (**16**) occurred rapidly (in time of mixing) at room temperature, suggesting that this type of V^{V}/V^{III} conproportionation reaction is kinetically viable.

One possibility is that coordination of pyridine to the vanadium center facilitates hydride transfer to the vanadium−oxo ligand. This is shown in path A, where initial coordination of pyridine to **1** is followed by a unimolecular reaction of **1-Pyr** to afford a vanadium(III) intermediate. Due to the observed rapid coordination and exchange of pyridine at room temperature and the primary kinetic isotope effect ($k_H/k_D = 5.7(5)$), the slow step of this pathway must be hydride transfer from the isopropoxide ligand of **1-Pyr** to the vanadium−oxo. Were the reaction proceeding by this pathway, electron-rich pyridines that coordinate more strongly to the vanadium center would promote faster hydride transfer than pyridines with electron-withdrawing substituents. The overall rate law for path A is shown in eq 6. At high pyridine concentrations, the rate law simplifies to eliminate the overall dependence on pyridine, as shown in eq 7. This is in conflict with the observed linear dependence of the reaction rate on pyridine at high pyridine concentrations, thus ruling out path A.

$$\text{path A:} \qquad \text{rate} = \frac{k_1 K_{eq}[V_t][pyr]}{1 + K_{eq}[pyr]} \tag{6}$$

$$\text{rate} = k_1[V_t] \tag{7}$$

A second possible reaction pathway (path B) entails rapid equilibrium coordination of pyridine to **1**, followed by a bimolecular reaction of **1-Pyr** with pyridine, where the C−H bond is broken in the rate-determining step. A bimolecular reaction with pyridine would be consistent with the experimentally determined negative entropy of activation ($\Delta S^{\ddagger} = -14(1)$ eu). The overall rate law for this pathway is depicted in eq 8. At high pyridine concentrations, the rate law simplifies to give a linear dependence on pyridine, as shown in eq 9. Path B would thus account for the linear dependence of the reaction rate on pyridine observed at high pyridine concentrations. However, the line fit to the experimental values of k_{obs} vs [pyridine] at high pyridine concentrations yields a positive *y*-intercept ($+1.1 \times 10^{-4}$) that would not be anticipated for path B. The observed positive *y*-intercept suggests that another pathway may be operating.

$$\text{path B:} \qquad \text{rate} = \frac{k_1 K_{eq}[pyr]^2[V_t]}{1 + K_{eq}[pyr]} \tag{8}$$

$$\text{rate} = k_1[pyr][V_t] \tag{9}$$

Path C is similar to path B, but in this mechanism both complexes **1** and **1-Pyr** undergo bimolecular reactions with pyridine to form the observed products. Path C would be consistent with the observed negative entropy of activation and

kinetic isotope effect. The rate law for path C is shown in eq 10. At high pyridine concentrations, the rate law simplifies as shown in eq 11, accounting for both the linear dependence on pyridine concentration and the positive *y*-intercept observed in the plot of k_{obs} vs [pyridine].

$$\text{path C:} \qquad \text{rate} = \frac{k_1[\text{pyr}][\text{V}_t]}{1 + K_{eq}[\text{Pyr}]} + \frac{k_2 K_{eq}[\text{pyr}]^2[\text{V}_t]}{1 + K_{eq}[\text{pyr}]} \tag{10}$$

$$\text{rate} = (k_1/K_{eq})[\text{V}_t] + k_2[\text{pyr}][\text{V}_t] \tag{11}$$

For path C, values of $K_{eq} = 2.2\ \text{M}^{-1}$, $k_1 = 3.1 \times 10^{-4}\ \text{M}^{-1}\ \text{s}^{-1}$, and $k_2 = 3.1 \times 10^{-5}\ \text{M}^{-1}\ \text{s}^{-1}$ can be obtained from a least-squares fit of the data to the overall rate law (eq 10). The value of $K_{eq} = 2.2\ \text{M}^{-1}$ (340 K) determined from the least-squares analysis of the kinetic data is in good agreement with $K_{eq} = 2(\pm 1)\ \text{M}^{-1}$ (340 K) determined from the ^{1}H NMR chemical shifts of **1** in the presence of varying pyridine concentration. Values of $k_1 = 3.1 \times 10^{-4}\ \text{M}^{-1}\ \text{s}^{-1}$ and $k_2 = 3.1 \times 10^{-5}\ \text{M}^{-1}\ \text{s}^{-1}$ determined from the least-squares fit of the rate law are also in good agreement with the slope (3.2×10^{-5}) and *y*-intercept ($+1.1 \times 10^{-4}$) of the line fit to k_{obs} vs [pyridine] at pyridine concentrations of 3−12.5 M (where the *y*-intercept $= k_1/K_{eq}$ and the slope $= k_2$).

While the experimental evidence supports pathway C, the precise nature of the C−H bond-breaking step remains somewhat ambiguous. The reaction is much faster with more basic pyridines, suggesting an attack of pyridine on the C−H bond. The reaction rate correlates well with the pK_a of the conjugate acid of the substituted pyridine, but also with σ, fitting a Hammett plot with $\rho = -2.5$. Jaffe and Fischer have shown that for 3- and 4-substituted pyridines, the acid dissociation reaction fits well to a Hammett plot, with pK_a for the pyridinium ion vs σ giving $\rho = 5.7$.[77,78] The magnitude of ρ for the reaction of **1** is less than 5.7, suggesting that the buildup of positive charge on the pyridine occurs to a lesser extent than in protonation.[79] The negative value of ρ demonstrates that electron-donating substituents on the pyridine accelerate the reaction. Electronic structure calculations to further clarify the nature of the transition state are currently underway; however, initial calculations are consistent with the observation of pyridine coordination to **1** and suggest that a pyridine-assisted pathway may be favored over an intramolecular H-atom abstraction.[80]

Varying the electronics of the dipic ligand has a significant impact on the rate of isopropanol oxidation, with HQC complex **8** reacting more slowly than **1** and dipicCl complex **6** reacting faster. However, in considering a complete catalytic cycle for the aerobic oxidation of alcohols, while electron-withdrawing ligands enhance the Lewis acidity of the vanadium center and facilitate the alcohol oxidation step, they also render the resulting vanadium(IV) complex more electron-deficient, and thus slow down the reaction of vanadium(IV) with oxygen to form vanadium(V). The development of more active catalysts will requiring balancing the electronic demands of the alcohol oxidation step with those required for regeneration of vanadium(V).

(77) Jaffe, H. H.; Doak, G. O. *J. Am. Chem. Soc.* **1955**, *77*, 4441–4444.
(78) Fischer, A.; Galloway, W. J.; Vaughan, J. *J. Chem. Soc.* **1964**, 3591–3596.
(79) Fischer, A.; Galloway, W. J.; Vaughan, J. *J. Chem. Soc.* **1964**, 3596–3599.
(80) Dong, H.; Hrovat, D.; Borden, W. T. Unpublished results.

Conclusions

Detailed investigations of the mechanism of alcohol oxidation by dipicolinate vanadium(V) have been carried out. The dipicolinate vanadium(V) isopropoxide complex **1** reacts cleanly with pyridine in acetonitrile or pyridine solution to generate the vanadium(IV) complex **9** and 0.5 equiv of acetone. Initial coordination of pyridine to **1** is rapid on the NMR time scale at room temperature, with $K_{eq} = 15(\pm 2)\ \text{M}^{-1}$ for the formation of **1-Pyr** at 298 K. Preparation of **1-*d*$_7$** allowed for determination of a primary kinetic isotope effect of 5.7(5) at 340 K, revealing that the C−H bond is broken in or before the rate-limiting step of the oxidation. Oxidations of the mechanistic probes cyclobutanol and α-*tert*-butylbenzyl alcohol have been studied and suggest a two-electron pathway proceeding through a vanadium(III) intermediate. Overall, the evidence points to a mechanism where both **1** and **1-Pyr** undergo a bimolecular reaction with pyridine to generate a vanadium(III) intermediate. Trends in the alcohol oxidation reaction have been established, with more basic pyridines reacting more rapidly. Increasing electron-donating ability of the ligand slows the alcohol oxidation reaction, with the relative order of reactivity dipicCl > dipic > dipicOMe > HQC.

Hydride transfer from a vanadium−alkoxide ligand to a vanadium−oxo ligand has been postulated as a key step in vanadium-mediated alcohol oxidation by Toste, Chen, and Uemura.[20,24−26] The involvement of pyridine in the elementary alcohol oxidation step determined for dipicolinate vanadium(V) is a substantial departure from what has been previously proposed and is a newly recognized type of mechanism for vanadium-mediated alcohol oxidation. Notably, the oxidation of benzylic and allylic alcohols reported by Ragauskas employs a nitrogen base (DABCO) co-catalyst, providing an indication that the involvement of base in the reaction of vanadium−alkoxide complexes is not limited to the dipicolinate system described here.[21,22] Using a base to promote alcohol oxidation could provide a new handle with which to tune reactivity of vanadium catalysts and could potentially even provide a means to control stereochemistry in alcohol oxidation reactions. Future studies will explore the generality of base-promoted alcohol oxidation and focus on the development of more effective vanadium alcohol oxidation catalysts.

Experimental Section

General Considerations. Unless specified otherwise, all reactions were carried out under a dry argon atmosphere using standard glovebox and Schlenk techniques. Pyridine-d_5, DMSO-d_6, D_2O, and CD_3CN were purchased from Cambridge Isotope Laboratories. Pyridine-d_5 and CD_3CN were dried over CaH_2. Anhydrous grade acetonitrile, pyridine, and diethyl ether were obtained from Fisher Scientific and used as received. 4-Nitrodipicolinic acid was purchased from ACES Pharma (Branford, CT), and 4-chlorodipicolinic acid was purchased from Small Molecules, Inc. (Hoboken, NJ). ^{1}H and ^{51}V NMR spectra were obtained at room temperature on a Bruker AV400 MHz spectrometer, with chemical shifts (δ) referenced to the residual solvent signal or referenced externally to $V^V(O)(Cl)_3$ (0 ppm). UV−vis spectra were obtained on an HP 8452A diode array spectrometer, and IR spectra were obtained on a Varian 1000 FT-IR Scimitar series or a Perkin-Elmer Spectrum One instrument. Elemental analyses were performed by Atlantic Microlab (Norcross, GA). (dipic)$V^V(O)(O^iPr)$ (**1**),[32] (dipic)-

$V^V(O)(OEt)$,[32] [(dipic)$V^V(O)_2$]HPy (**15**),[35] and [(dipic)V(pyridine)$_2$]$_2$(μ-O) (**16**)[35] were prepared according to published procedures. 4-Methoxydipicolinic acid was prepared by base-catalyzed hydrolysis of 4-methoxypyridine-2,6-dicarboxylic acid dimethyl ester[33] according to a published procedure.[34]

(dipic)V^V(O)(O^iPr)-d_7 (1-d_7). Complex **1** (0.208 g, 0.593 mmol) and isopropanol-d_8 (0.350 g, 5.15 mmol) were dissolved in CH_3CN (4 mL). The mixture was stirred at room temperature for 5−10 min, and then the solvent was removed under vacuum. The yellow residue was dissolved in CH_3CN (2 mL), and more isopropanol-d_8 (0.590 g, 8.68 mmol) was added. The solvent was removed again under vacuum, leaving a pale yellow solid. Yield: 0.214 g (99%). Integration of the ^{1}H NMR spectrum of the yellow solid indicated that the extent of deuteration in the isopropoxide ligand was approximately 93%.

(dipic)V^V(O)(OBu) (2). In a vial, (dipic)V(O)O^{i}Pr (0.166 g, 0.472 mmol) and 1-butanol (0.360 g, 4.86 mmol) were suspended in CH_3CN (2 mL). The solution was stirred for approximately 5 min, during which time all of the solid dissolved. The solvent was removed under vacuum, leaving a yellow residue. The yellow residue was then stirred with diethyl ether (8 mL), yielding a yellow suspension. The yellow solid was allowed to settle, and the supernatant was removed by pipet. The resulting yellow solid was washed with diethyl ether (5 mL) and then dried under vacuum. Integration of the ^{1}H NMR spectrum of the yellow solid product indicated that the complex co-crystallized with 1 equiv of 1-butanol. Yield: 0.124 g (70%). ^{1}H NMR (CD_3CN, 400 MHz): δ 8.56 (t, 1H, J = 7.6 Hz, Py), 8.23 (d, 2H, J = 7.6 Hz, Py), 5.99 (t, 2H, J = 6.4 Hz, V-OCH_2), 3.47 (t, 2H, J = 6.4 Hz, 1-butanol), 1.99 (m, 2H, V-butanoxide), 1.58 (sextet, 2H, J = 7.6 Hz, V-butanoxide), 1.43 (m, 2H, 1-butanol), 1.32 (sextet, 2H, J = 7.6 Hz, 1-butanol), 1.03 (t, 3H, J = 7.2 Hz, V-butanoxide), 0.895 (t, 3H, J = 7.6 Hz, 1-butanol). ^{51}V NMR (CD_3CN, 105 MHz): −569.5 (s). IR (thin film): $\nu_{C=O}$ = 1682 cm^{-1}, $\nu_{V=O}$ = 990 cm^{-1}. Anal. Calcd for $C_{15}H_{22}NO_7V$: C, 47.50; H, 5.85; N, 3.69. Found: C, 47.49; H, 5.75; N, 3.77.

(dipic)V(O)(OCyBu) (3). (dipic)V^V(O)(OEt) (0.1655 g, 0.512 mmol) and cyclobutanol (0.1534 g, 2.131 mmol) were dissolved in CH_3CN (3 mL), forming a yellow-orange solution. The solution was allowed to stand at room temperature for 5−10 min, and then the solvent was removed under vacuum. The resulting yellow-orange solid was redissolved in CH_3CN (1.25 mL) containing cyclobutanol (0.160 g, 2.22 mmol). Orange-yellow crystals of **3** were obtained by slow diffusion of diethyl ether at −15 °C; complex **3** co-crystallized with 1 equiv of cyclobutanol. Yield: 0.136 g (71%). ^{1}H NMR (CD_3CN, 400 MHz): δ 8.57 (t, 1H, J = 7.6 Hz, Pyr), 8.23 (d, 2H, J = 7.6 Hz, Pyr), 6.41 (m, 1H, V-OCH), 4.06 (m, 1H, cyclobutanol), 2.79−2.72 (m, 2H, V-cyclobutanoxide), 2.63−2.53 (m, 2H, V-cyclobutanoxide), 2.19−2.13 (m, 2H, cyclobutanol), 1.90−1.66 (m, 4H, V-cyclobutanoxide, cyclobutanol), 1.61−1.54 (m, 1H, cyclobutanol), 1.45−1.36 (m, 1H, cyclobutanol). ^{51}V NMR (CD_3CN, 105 MHz): −571.4 (s). IR (thin film): $\nu_{C=O}$ = 1685 cm^{-1}, $\nu_{V=O}$ = 991 cm^{-1}.

(dipic)V^V(O)(TBA) (4). In a vial, α-*tert*-butylbenzyl alcohol (0.218 g, 1.35 mmol) was dissolved in CH_3CN (3 mL). Calcium hydride (0.030 g, 0.71 mmol) was added, and the suspension was stirred at room temperature for 3 h. The solution was filtered through a Teflon syringe filter into a second vial containing (dipic)V(O)(O^{i}Pr) (0.134 g, 0.382 mmol). The mixture was stirred at room temperature for 20 min, forming a yellow solution. The solvent was subsequently removed under vacuum, leaving a yellow residue. CH_3CN (3 mL) was added, and the resulting yellow suspension was stirred at room temperature for 20 min. The solvent was again removed under vacuum, leaving a yellow oily residue. Diethyl ether (15 mL) was added, forming a yellow slurry, which was stirred for 2 h at room temperature. The yellow solid was collected on a frit, washed with diethyl ether (3 × 1 mL), and dried under vacuum. Yield: 0.183 g (86%). ^{1}H NMR (CD_3CN, 400 MHz): δ 8.55 (t, 1H, J = 7.6 Hz, Py), 8.23 (d, 1H, J = 7.6 Hz, Py), 8.20 (d, 1H, J = 7.6 Hz, Py), 7.44−7.37 (m, 5H, V-OCH-Ph), 7.31−7.23 (m, 5H, α-*tert*-butylbenzyl alcohol), 7.15 (s, 1H, V-OCH), 4.32 (s, 1H, α-*tert*-butylbenzyl alcohol), 1.07 (s, 9H, V-OC(C(CH_3)$_3$), 0.87 (s, 9H, α-*tert*-butylbenzyl alcohol). ^{51}V NMR (CD_3CN, 105 MHz): −579.0 (s). IR (thin film): $\nu_{C=O}$ = 1690 cm^{-1}, $\nu_{V=O}$ = 988 cm^{-1}.

(dipicNO_2)V^V(O)(O^iPr) (5). 4-Nitrodipicolinic acid (0.223 g, 1.05 mmol) was suspended in isopropanol (8 mL), and V^V(O)(O^{i}Pr)$_3$ (248 μL, 1.05 mmol) was added. The reaction mixture was stirred at room temperature for 4 h, during which time a yellow precipitate formed. The yellow solid was collected on a frit, washed with diethyl ether (3 × 1 mL), and dried under vacuum. Yield: 0.320 g (90%). Integration of the ^{1}H NMR spectrum of the yellow solid product indicated that the complex co-crystallized with 0.5 equiv of isopropanol. Anal. Calcd for [(dipicNO_2)V^V(O)O^{i}Pr]$_2$·^{i}PrOH $C_{23}H_{26}N_4O_{17}V_2$: C, 47.50; H, 5.85; N, 3.69. Found: C, 47.49; H, 5.75; N, 3.77. ^{1}H NMR (CD_3CN, 400 MHz): δ 8.80 (s, 2H, Py), 6.51 (h, 1H, J = 6.0 Hz, V-OCH), 3.86 (h, 1H, J = 6.0 Hz, isopropanol), 2.55 (s, 1H, isopropanol OH), 1.68 (d, 6H, J = 6.0 Hz, V-isopropoxide), 1.08 (d, 6H, J = 6.0 Hz, isopropanol). ^{51}V NMR (CD_3CN, 105 MHz): −588.2 (s). IR (thin film): $\nu_{N=O}$ = 1553 cm^{-1}, 1366 cm^{-1}, $\nu_{C=O}$ = 1695 cm^{-1}, $\nu_{V=O}$ = 992 cm^{-1}.

(dipicCl)V^V(O)(O^iPr) (6). 4-Chlorodipicolinic acid (0.263 g, 1.31 mmol) was dissolved in methanol (10 mL). The solution was filtered through a Teflon syringe filter to remove a fine brown solid, and the solvent was removed under vacuum. The remaining solid was then suspended in isopropanol (8 mL), and V^V(O)(O^{i}Pr)$_3$ (294 μL, 1.25 mmol) was added. The reaction mixture was stirred for 4 h at room temperature, forming a light tan suspension. The tan solid was collected on a frit, washed with diethyl ether (2 × 2 mL), and dried under vacuum. The crude product was then recrystallized by dissolving in CH_3CN (2 mL), filtering through a glass wool pipet, and cooling to −20 °C overnight. The yellow crystals were washed with diethyl ether (2 × 2 mL) and dried under vacuum. Yield: 0.0926 g (23%). ^{1}H NMR (CD_3CN, 400 MHz): δ 8.28 (s, 2H, Py), 6.39 (h, 1H, J = 6.0 Hz, V-OCH), 1.66 (d, 6H, J = 6.0 Hz, V-isopropoxide). ^{51}V NMR (CD_3CN, 105 MHz): −588.9 (s). IR (thin film): $\nu_{C=O}$ = 1694 cm^{-1}, $\nu_{V=O}$ = 990 cm^{-1}. Anal. Calcd for $C_{10}H_9ClNO_6V$: C, 37.72; H, 3.58; N, 7.65. Found: C, 37.78; H, 3.54; N, 7.81.

(dipicOMe)V^V(O)(O^iPr) (7). 4-Methoxydipicolinic acid (0.028 g, 0.14 mmol) was suspended in isopropanol (2 mL). V^V(O)(O^{i}Pr)$_3$ (34 μL, 0.14 mmol) was added, and the reaction mixture was stirred for 20 min at room temperature, forming a yellow suspension. Diethyl ether (6 mL) was added, and the mixture was cooled to −20 °C overnight. The supernatant was removed by pipet, and the yellow powder washed with diethyl ether (3 mL) and dried under vacuum. Integration of the ^{1}H NMR spectrum of the yellow solid product indicated that the complex co-crystallized with 0.5 equiv of isopropanol. Yield: 0.038 g (84%). ^{1}H NMR (CD_3CN, 400 MHz): δ 7.65 (s, 2H, Py), 6.22 (h, 1H, J = 6.0 Hz, V-OCH), 3.86 (h, 1H, J = 6.0 Hz, isopropanol), 1.66 (d, 6H, J = 6.4 Hz, V-isopropoxide), 1.08 (d, 6H, J = 6.0 Hz, isopropanol). ^{51}V NMR (CD_3CN, 105 MHz): −590.3 (s). IR (thin film): $\nu_{C=O}$ = 1683 cm^{-1}, $\nu_{V=O}$ = 991 cm^{-1}.

(HQC)V^V(O)(O^iPr) (8). In a vial, V^V(O)(O^{i}Pr)$_3$ (250 μL, 1.07 mmol) was added to a suspension of 8-hydroxyquinoline-2-carboxylic acid (0.2016 g, 1.07 mmol) in CH_3CN (6 mL). The mixture was stirred at room temperature for 20 min, forming a dark red solution. Cooling the solution overnight (−20 °C) yielded a dark red solid. The supernatant was removed by pipet, and the red solid was washed with diethyl ether (2 × 5 mL) and dried under vacuum. Yield: 0.188 g (56%). ^{1}H NMR (CD_3CN, 400 MHz): δ 8.82 (d, 1H, J = 8.4 Hz, HQC), 8.02 (d, 1H, J = 8.8 Hz, HQC), 7.76 (t, 1H, J = 8.0 Hz, HQC), 7.54 (d, 1H, J = 8.4 Hz, HQC), 7.05 (d, 1H, J = 7.6 Hz, HQC), 6.07 (h, 1H, J = 6.0 Hz, V-OCH), 1.69 (overlapping doublets, 6H, J = 8.0 Hz, V-isopropoxide). ^{51}V NMR (CD_3CN, 105 MHz): −549.8 (s). IR (thin film): $\nu_{C=O}$ = 1702 cm^{-1}, $\nu_{V=O}$ = 990 cm^{-1}. Anal. Calcd for $C_{13}H_{12}NO_5V$: C, 49.86; H, 3.86; N, 4.47. Found: C, 50.29; H, 3.74; N, 4.68.

Table 4. Crystallographic Data Collection Parameters for **1-Pyr** and **11**

	(dipic)V^{V}(O)(O^{i}Pr)(pyr) (**1-Pyr**)	(HQC)V^{IV}(O)$(DMSO)_2$ (**11**)
empirical formula	$C_{16}H_{15}N_2O_3V$	$C_{14}H_{17}NO_6S_2V$
FW	334.24	410.35
T (K)	140(1)	140(1)
wavelength (Å)	0.71073	0.71073
crystal description	yellow block	brown needle
space group	$P2_1/c$	$P2_1/c$
unit cell dimensions	$a = 8.9203(10)$	$a = 14.241(5)$
(Å, deg)	$b = 15.9259(19)$	$b = 8.419(3)$
	$c = 11.4477(13)$	$c = 15.213(5)$
	$\alpha = 90$	$\alpha = 90$
	$\beta = 92.305(13)$	$\beta = 112.926(3)$
	$\gamma = 90$	$\gamma = 90$
V (Å^3)	1625.0(3)	1679.8(10)
Z, ρ (Mg/m^3)	4, 1.366	4, 1.623
μ (mm^{-1})	0.623	0.869
F(000)	688	844
crystal size	0.14 × 0.10 × 0.08 mm	0.24 × 0.20 × 0.08 mm
θ range (deg)	2.19−25.35	2.71−25.34
index ranges	$-10 \le h \le 10$	$-17 \le h \le 17$
	$0 \le k \le 19$	$-10 \le k \le 10$
	$0 \le l \le 13$	$-18 \le l \le 18$
reflections collected, unique	15962, 6026 [R(int) = 0.0652]	15195, 3064 [R(int) = 0.0490]
completeness to θ (%)	100.0	99.9%
refinement method	full-matrix least-squares on F^2	full-matrix least-squares on F^2
goodness of fit on F^2	$S = 0.793$	$S = 1.307$
R_1 ($I > 2\sigma$)	0.0348	0.0373
wR ($I > 2\sigma$)	0.0761	0.1039

(HQC)V^{IV}(O)$(pyr)_2$ (10). In a small glass vessel equipped with a Teflon stopcock, (HQC)V^{V}(O)(O^{i}Pr) (0.101 g, 0.322 mmol) was dissolved in pyridine (2 mL). The solution was heated at 80 °C for 1 h. The volume of the pyridine was reduced to ∼0.5 mL under vacuum, and the solution was allowed to stand at room temperature for 4 days. The solution was then cooled to −20 °C, yielding green/brown crystals. The supernatant was decanted, and the crystals were washed with diethyl ether (1 × 6 mL) and dried under vacuum. Yield: 0.092 g (70%). IR (pyridine solution): $\nu_{C=O} = 1672$ cm^{-1}, $\nu_{V=O} = 957$ cm^{-1}. UV−vis (pyridine): $\lambda = 380$ nm, $\varepsilon = 3600$ M^{-1} cm^{-1}; $\lambda = 350$ nm, $\varepsilon = 3900$ M^{-1} cm^{-1}. Anal. Calcd for $C_{20}H_{15}N_3O_4V$: C, 58.26; H, 3.67; N, 10.19. Found: C, 57.12; H, 3.70; N, 10.26.

(HQC)V^{IV}(O)$(DMSO)_2$ (11). Complex **10** (0.040 g, 0.097 mmol) was dissolved in DMSO (0.6 mL). Slow diffusion of diethyl ether at room temperature yielded crystals of **11** suitable for X-ray diffraction. IR (DMSO solution): $\nu_{C=O} = 1657$ cm^{-1}, $\nu_{V=O} = 950$ cm^{-1}. UV−vis (DMSO): $\lambda = 406$ nm, $\varepsilon = 2200$ M^{-1} cm^{-1}; $\lambda = 348$ nm, $\varepsilon = 2300$ M^{-1} cm^{-1}. X-ray data are given in Table 4.

(dipicOMe)V^{IV}(O)$(pyr)_2$ (12). In a small, thick-walled glass vessel equipped with a Teflon stopcock, complex **7** (0.022 g, 0.069 mmol) was dissolved in pyridine (1 mL). The mixture was heated at 100 °C for 1 h and then cooled to room temperature, and the volume of the solvent was reduced to ∼0.25 mL under vacuum. Green crystals formed upon cooling to −20 °C overnight. The supernatant was removed by pipet, and the crystals were washed with diethyl ether (2 × 1 mL) and dried under vacuum. Yield: 0.0176 g (76%). IR (pyridine solution): $\nu_{C=O} = 1673$ cm^{-1}, $\nu_{V=O} = 960$ cm^{-1}. UV−vis (pyridine): $\lambda = 346$ nm, $\varepsilon = 700$ M^{-1} cm^{-1}. Anal. Calcd for $C_{18}H_{15}N_3O_6V$: C, 51.44; H, 3.60; N, 10.00. Found: C, 50.14; H, 3.30; N, 9.73.

[(dipicNO_2)$V^{V}$$(O)_2$]HPy (14). Complex **5** (38.9 mg, 0.116 mmol) was dissolved in pyridine (1 mL), forming a yellow solution. Within minutes, the solution turned cloudy, and a tan solid precipitate formed. After 20 min, the tan precipitate was collected on a frit, washed with diethyl ether (2 × 1 mL), and dried under vacuum. Yield: 0.0224 g (52%). ^{1}H NMR (DMSO-d_6, 400 MHz): δ 9.52 (d, 2H, $J = 5.6$ Hz, HPyr), 8.91 (t, 1H, $J = 7.2$ Hz, HPyr), 8.85 (s, 2H, dipicNO_2), 8.41 (t, 1H, $J = 6.8$ Hz, HPyr). ^{51}V NMR (DMSO-d_6, 105 MHz): −518.0 (s). NMR data in D_2O were consistent with those reported for [(dipicNO_2)$V^{V}$$(O)_2$]K.[40]

Thermolysis of (dipic)V^{V}(O)(O^{i}Pr) (1) in CD_3CN. In a resealable Teflon-capped NMR tube, complex **1** (4.2 mg, 0.012 mmol) was dissolved in CD_3CN (0.6 mL) containing 1,3,5-tri-*tert*-butylbenzene (2.0 mM) as an internal standard. An initial ^{1}H NMR spectrum was recorded, and then the solution was heated at 100 °C. After heating of the solution for 3 weeks, integration of the ^{1}H NMR spectrum revealed that only ∼20% of **1** had reacted, forming acetone in ca. 12% yield.

Thermolysis of (dipic)V^{V}(O)(OBu) (2) in Pyridine-d_5. In a resealable Teflon-capped NMR tube, complex **2** (5.0 mg, 0.013 mmol) was dissolved in pyr-d_5 (0.6 mL) containing ethyl acetate (3.7 mM) as an internal standard. An initial ^{1}H NMR spectrum was recorded, and then the reaction was heated at 100 °C for 30 min. The solution was cooled to room temperature, and integration of the ^{1}H NMR spectrum revealed formation of butyraldehyde in 80% yield. The NMR and IR spectra of the solution were consistent with the formation of **9**.

Thermolysis of (dipic)V^{V}(O)(OCyBu) (3) in Pyridine-d_5. In an NMR tube, cyclobutanoxide complex **3** (4.0 mg, 0.013 mmol) was dissolved in pyridine-d_5 (0.6 mL) containing diethyl ether (12 mM) as an internal standard. The reaction was heated at 100 °C for 30 min, resulting in a color change from yellow-orange to green. Examination of the ^{1}H NMR spectrum of the reaction mixture revealed formation of cyclobutanone; a 93% yield was determined by the average of four runs of this type. Performing the reaction on a larger scale (26 mg) allowed for the isolation of 25.4 mg of green crystals. Elemental analysis (found: C, 52.66; H, 3.49; N, 10.41) and the UV−vis spectrum of this material agreed with formulation as (dipic)V^{IV}(O)$(pyr)_2$ (**9**) (94% yield).

Thermolysis of (dipic)V^{V}(O)(TBA) (4) in Pyridine-d_5. In a resealable Teflon-capped NMR tube, complex **4** (6.8 mg, 0.012 mmol) was dissolved in pyr-d_5 (0.6 mL) containing diethyl ether (12 mM) as an internal standard. An initial ^{1}H NMR spectrum was recorded, and the solution was heated at 100 °C for 20 min, resulting in a color change from yellow to green. Integration against the internal standard revealed that 2,2-dimethylpropiophenone was formed in 98% yield. Spiking the reaction mixture with a commercial sample of 2,2-dimethylpropiophenone confirmed the identity of this product. When a similar reaction was carried out in the presence of 9,10-dihydroanthracene (0.051 M), no formation of anthracene was detected by ^{1}H NMR.

Reaction of 4 in CD_3CN. In a resealable Teflon-capped NMR tube, complex **4** (4.5 mg, 8.1 μmol) was dissolved in CD_3CN (0.6 mL) containing THF (3.6 mM) as an internal standard. An initial ^{1}H NMR spectrum was recorded, and then the solution was allowed to stand in ambient light at room temperature. After 9 days, a green precipitate had formed, and integration of the ^{1}H NMR spectrum revealed the formation of benzaldehyde (92%) and *tert*-butanol (74%), as well as several minor unidentified products resulting from the *tert*-butyl moiety. When the reaction was conducted in CH_3CN (1 mL) on a slightly larger scale (16.5 mg of **4**), 6.6 mg of the green solid product was isolated after washing with diethyl ether (1 mL) and drying under vacuum. Dissolution of this material in pyr-d_5 showed a peak corresponding to CH_3CN, and the ^{1}H NMR and IR spectra were consistent with (dipic)V^{IV}(O)(pyr)$_2$.

The reaction of complex **4** (3.9 mg, 7.0 μmol) was also followed in CD_3CN (0.6 mL) in the presence of 9,10-dihydroanthracene (5.4 mg, 30 μmol) and a THF (9.0 mM) internal standard. After 9 days, integration of the ^{1}H NMR spectrum revealed that anthracene had formed in 12% yield (based on the oxidizing equivalents of vanadium consumed).

Thermolysis of (dipicCl)V^V(O)(O^{i}Pr) (6) in Pyridine-d_5. In a resealable Teflon-capped NMR tube, complex **6** (13.4 mg, 0.0412 mmol) was dissolved in pyr-d_5 (0.6 mL) containing diethyl ether (0.037 M) as an internal standard. The reaction mixture was heated at 100 °C for 30 min, during which time a green-brown precipitate formed. The precipitate was allowed to settle, at which time integration of the ^{1}H NMR spectrum revealed the complete consumption of **6** and formation of acetone (0.5 equiv, 100% yield). The green solid was transferred to a vial, washed with diethyl ether (2 × 0.5 mL), and dried under vacuum. Yield: 0.0156 g (89%). The IR spectrum of this material (Nujol mull, $\nu_{C=O}$ = 1660 cm^{-1}, $\nu_{V=O}$ = 962 cm^{-1}) and elemental analysis (found: C, 47.14; H, 3.01; N, 9.32) were consistent with formulation as (dipicCl)-V^{IV}(O)(pyr)$_2$.

Thermolysis of (HQC)V^V(O)(O^{i}Pr) (8) in Pyridine-d_5. In a resealable Teflon-capped NMR tube, complex **8** (5.0 mg, 0.016 mmol) was dissolved in pyr-d_5 (0.6 mL) containing diethyl ether (0.034 M) as an internal standard. An initial ^{1}H NMR spectrum was recorded, and then the solution was heated at 100 °C for 2.5 h, during which time the color changed from dark red to yellow. After the solution was cooled to room temperature, examination of the ^{1}H NMR spectrum revealed formation of acetone (0.5 equiv, 90% yield).

Conproportionation of [(dipic)V^V(O)$_2$]HPyr (15) and [(dipic)-V^{III}(pyridine)$_2$]$_2$(μ-O) (16). Complex **15** (4.2 mg, 0.0128 mmol) and complex **16** (5.1 mg, 0.0067 mmol) were combined in a small vial. Pyridine (1.5 mL) was added, and the solution was mixed at room temperature. Within the time of mixing, the dark purple color of **16** faded, forming a green solution. Both the IR ($\nu_{C=O}$ = 1677 cm^{-1}, $\nu_{V=O}$ = 964 cm^{-1}) and UV−vis spectra of the solution were consistent with quantitative formation of (dipic)V^{IV}(O)(pyr)$_2$ (**9**).

General Procedure for the Determination of the Equilibrium Constant for Coordination of Pyridine to 1. In a resealable Teflon-capped NMR tube, complex **1** (ca. 6 mg, 0.017 mmol) was dissolved in CD_3CN (0.6 mL). Pyridine was added in increments of 5−60 μL, over a concentration range of 0−3.5 M, and ^{1}H and ^{51}V NMR spectra were recorded after each addition. The changes in ^{51}V NMR chemical shift or ^{1}H NMR chemical shift (isopropyl methine proton) were used to calculate K_{eq} according to eqs 2 and 3, using Excel to perform a least-squares fit to the data. Values of K_{eq} for the coordination of pyridine were determined from the average of two independent titration experiments of this type. Analogous titrations were conducted with 4-cyanopyridine, 2,6-lutidine, and 2,6-di-*tert*-butylpyridine.

General Procedure for Kinetic Studies. Complex **1** (ca. 6 mg, 0.017 mmol) was weighed into a resealable Teflon-capped NMR tube. The complex was dissolved in pyr-d_5 (0.6 mL) or CD_3CN/pyr-d_5 (0.6 mL total volume), and an internal standard was added (THF, dioxane, or diethyl ether). The reaction was heated in the probe of a Bruker AV400 MHz spectrometer, where the temperature was calibrated using an ethylene glycol standard. ^{1}H NMR spectra were recorded at intervals, and the disappearance of complex **1** was followed by integration against the internal standard. Rate constants were determined by monitoring the reaction through at least three half-lives. For the reactions of **1** with 4-trifluoromethylpyridine and 4-cyanopyridine, the reactions at 340 K were too slow to monitor in the NMR probe. The NMR tubes were instead heated in a temperature-controlled IKA oil bath and monitored periodically by ^{1}H NMR spectroscopy.

Acknowledgment. This work was supported by Los Alamos National Laboratory LDRD (ER 20100160 and Director's PD Fellowship to S.K.H.) and NSF via the Center for Enabling New Technologies through Catalysis (CENTC). We thank Professors W. T. Borden (UNT), D. Hrovat (UNT), S. L. Scott (UCSB), and P. C. Ford (UCSB) for helpful discussions and collaborations, and Dr. P. C. Stark (LANL) for help with instrumentation.

Supporting Information Available: Additional kinetic plots, rate law derivations, X-ray structure of **12**, and CIF files for **1-Pyr** and **11**. This material is available free of charge via the Internet at http://pubs.acs.org.

JA105739K